

Amplitude Analysis of the Decay $\bar{B}^0 \rightarrow K_S^0 \pi^+ \pi^-$ and First Observation of the CP Asymmetry in $\bar{B}^0 \rightarrow K^*(892)^- \pi^+$

R. Aaij *et al.**
(LHCb collaboration)

 (Received 8 January 2018; revised manuscript received 15 March 2018; published 25 June 2018)

The time-integrated untagged Dalitz plot of the three-body hadronic charmless decay $\bar{B}^0 \rightarrow K_S^0 \pi^+ \pi^-$ is studied using a pp collision data sample recorded with the LHCb detector, corresponding to an integrated luminosity of 3.0 fb^{-1} . The decay amplitude is described with an isobar model. Relative contributions of the isobar amplitudes to the $\bar{B}^0 \rightarrow K_S^0 \pi^+ \pi^-$ decay branching fraction and CP asymmetries of the flavor-specific amplitudes are measured. The CP asymmetry between the conjugate $\bar{B}^0 \rightarrow K^*(892)^- \pi^+$ and $B^0 \rightarrow K^*(892)^+ \pi^-$ decay rates is determined to be -0.308 ± 0.062 .

DOI: [10.1103/PhysRevLett.120.261801](https://doi.org/10.1103/PhysRevLett.120.261801)

The breaking of the invariance of the weak interaction under the combined action of the charge conjugation (C) and parity (P) transformations is firmly established in the K - and B -meson systems [1–3]. In particular, significant CP asymmetries at the level of 10% or more have been measured in the decays of B mesons into two light pseudoscalars. The CP asymmetries in the decays of $\bar{B}^0 \rightarrow K^- \pi^+$ and $B^- \rightarrow K^- \pi^0$ (CP conjugation is implied in the notation of the decays unless stated otherwise) are observed to be different [4], while, in predictions based on the QCD factorization approach, the two asymmetries are expected to be similar [5]. This apparent discrepancy is often referred to in the literature as the $K\pi$ puzzle [6–9]. The study of the flavor-specific, quasi-two-body amplitudes that contribute to the decay $\bar{B}^0 \rightarrow K_S^0 \pi^+ \pi^-$ offers the possibility to measure CP asymmetries. In particular, the decays with a vector and a pseudoscalar in the final state, such as $\bar{B}^0 \rightarrow K^*(892)^- \pi^+$, may help to shed light on the $K\pi$ puzzle.

The decay $\bar{B}^0 \rightarrow K_S^0 \pi^+ \pi^-$ can also proceed via CP -eigenstates, such as $\bar{B}^0 \rightarrow f_0(980)K_S^0$ or $\bar{B}^0 \rightarrow \rho(770)^0 K_S^0$. In the standard model (SM) [10,11], the mixing-induced CP asymmetries in the quark-level transitions $b \rightarrow q\bar{q}s$ ($q = u, d, s$), which govern the decay $\bar{B}^0 \rightarrow K_S^0 \pi^+ \pi^-$, are predicted to be approximately equal to those in $b \rightarrow c\bar{c}s$ transitions, such as $B^0 \rightarrow J/\psi K_S^0$. The existence of new particles in extensions of the SM could introduce additional weak phases that contribute along with the SM mixing

phase [12–15]. In general, for each of the studied CP eigenstates, the current experimental measurements of $b \rightarrow q\bar{q}s$ decays [4] show good agreement with the results from $b \rightarrow c\bar{c}s$ decays [4]. There is nonetheless room for contributions from physics beyond the SM and, hence, the need for precision measurements of these weak mixing phases.

The mixing-induced CP -violating phase can be measured by means of a decay-time-dependent analysis of the Dalitz plot (DP) [16] of the decay $\bar{B}^0 \rightarrow K_S^0 \pi^+ \pi^-$ [17–20]. Such an analysis requires the initial flavor of the \bar{B}^0 meson to be determined or “tagged.” A recent study of the yields of the charmless three-body decays $\bar{B}^0 \rightarrow K_S^0 \pi^+ \pi^-$ has been reported in Ref. [21]. The $\bar{B}^0 \rightarrow K_S^0 \pi^+ \pi^-$ yields are comparable to those obtained at the *BABAR* and *Belle* experiments, but the lower tagging efficiency at LHCb does not yet allow a precise flavor-tagged analysis to be performed. The decay-time-integrated untagged DP of this mode is studied in this Letter. The DP of the decay $\bar{B}^0 \rightarrow K_S^0 \pi^+ \pi^-$ is modeled by a sum of quasi-two-body amplitudes (the isobar parametrization), and the model is fit to the LHCb data to measure the relative branching fractions and the CP asymmetries of flavor-specific final states.

The analysis reported in this Letter is performed using pp collision data recorded with the LHCb detector, corresponding to integrated luminosities of 1.0 fb^{-1} at a center-of-mass energy of 7 TeV in 2011 and to 2.0 fb^{-1} at a center-of-mass energy of 8 TeV in 2012. The LHCb detector [22,23] is a single-arm forward spectrometer covering the pseudorapidity range $2 < \eta < 5$, designed for the study of particles containing b or c quarks. Signal candidates are accepted if one of the final-state particles from the signal decay deposits sufficient energy transverse to the beam line in the hadronic calorimeter to pass the hardware trigger. Events that are triggered at the hardware level by another particle in the event are also

*Full author list given at the end of the article.

Published by the American Physical Society under the terms of the [Creative Commons Attribution 4.0 International license](https://creativecommons.org/licenses/by/4.0/). Further distribution of this work must maintain attribution to the author(s) and the published article's title, journal citation, and DOI. Funded by SCOAP³.

retained. In a second step, a software trigger requires a two-, three-, or four-track secondary vertex with a significant displacement from any primary pp interaction vertex (PV). At least one charged particle must have a large transverse momentum and be inconsistent with originating from a PV. A multivariate algorithm [24] is used for the identification of secondary vertices consistent with the decay of a b hadron.

The selection procedure is described in detail in Ref. [21]. Decays of $K_S^0 \rightarrow \pi^+\pi^-$ are reconstructed in two different categories: the first involving K_S^0 mesons that decay early enough for the resulting pions to be reconstructed in the vertex detector; and the second containing those K_S^0 mesons that decay later, such that track segments of the pions cannot be formed in the vertex detector. These categories are referred to as Long and Downstream, respectively. Downstream K_S^0 were not reconstructed in the software trigger in 2011, but they were reconstructed and used for triggering in 2012. Furthermore, an improved software trigger with larger b -hadron efficiency, in particular in the Downstream category, was used for the second part of the 2012 data taking. To take into account the different levels of trigger efficiency, the data sample is divided into 2011, 2012a, and 2012b data-taking periods, and each period is further divided according to the K_S^0 reconstruction category, giving a total of six subsamples. The 2012b sample is the largest, corresponding to an integrated luminosity 1.4 fb^{-1} , and it has the highest trigger efficiency.

The events passing the trigger requirements are then filtered in two stages. Initial requirements are applied to further reduce the size of the data sample and increase the signal purity, before a multivariate classifier, based mostly on topological variables derived from the vertexing of the candidates, is implemented [21]. The selection requirement placed on the output of the multivariate classifier is defined for each data subsample to yield a signal purity close to 90%. Particle identification (PID) requirements are applied in order to reduce backgrounds from decays where either a proton, kaon, or muon is misidentified as a pion. These criteria are optimized to reduce the cross-feed background coming from the decays $B_s^0 \rightarrow K_S^0 K^\pm \pi^\mp$, where the kaon is misidentified as a pion. The same invariant-mass vetoes on charmed and charmonium resonances as in Ref. [21] are used in this analysis. The invariant-mass distribution of signal candidates from the six aforementioned subsamples is displayed in Fig. 1, with the result of a simultaneous fit. The candidates selected for the subsequent DP analysis are those in the $K_S^0 \pi^+ \pi^-$ mass range $[5227, 5343] \text{ MeV}/c^2$.

The DP analysis technique [16] is employed to study the dynamics of the three-body decay $\bar{B}^0 \rightarrow K_S^0 \pi^+ \pi^-$. A decay-time-integrated untagged probability density function (PDF) is built to describe the phase space of the decay as a function of the DP kinematical variables. Neglecting

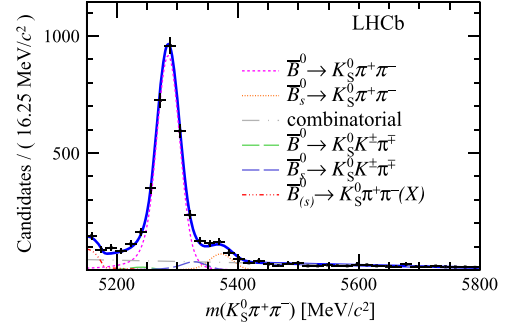


FIG. 1. Invariant mass distributions of $K_S^0 \pi^+ \pi^-$ candidates, summing the two years of data taking and the two K_S^0 reconstruction categories. The sum of the partially reconstructed contributions from B to open charm decays, charmless hadronic decays, $\bar{B}^0 \rightarrow \eta' K_S^0$, and charmless radiative decays are denoted $\bar{B}_{(s)}^0 \rightarrow K_S^0 \pi^+ \pi^- (X)$. Signal candidates for the Daltz plot analysis are those in the $K_S^0 \pi^+ \pi^-$ mass range $[5227, 5343] \text{ MeV}/c^2$.

the unobserved to date CP violation in $B^0 - \bar{B}^0$ mixing, the untagged PDF describing the signal does not exhibit any dependence on the mixing parameters [4,25], and it simply reduces to an incoherent sum of the $\mathcal{A}(s_+, s_-)$ and $\bar{\mathcal{A}}(s_+, s_-)$ Lorentz-invariant transition amplitudes of the decays $B^0 \rightarrow K_S^0 \pi^+ \pi^-$ and $\bar{B}^0 \rightarrow K_S^0 \pi^+ \pi^-$, respectively.

$$\mathcal{P}(s_+, s_-) = \frac{|\mathcal{A}(s_+, s_-)|^2 + |\bar{\mathcal{A}}(s_+, s_-)|^2}{\iint_{\text{DP}} (|\mathcal{A}(s_+, s_-)|^2 + |\bar{\mathcal{A}}(s_+, s_-)|^2) ds_+ ds_-}, \quad (1)$$

where the kinematical variables s_{\pm} denote the mass squared, $m_{K_S^0 \pi^\pm}^2$.

The total amplitude $\bar{\mathcal{A}}(s_+, s_-)$ of the decay $\bar{B}^0 \rightarrow K_S^0 \pi^+ \pi^-$ is described as a coherent sum of the amplitudes of possible intermediate resonances and nonresonant contributions. The decay amplitudes for B^0 and \bar{B}^0 are given by

$$\mathcal{A} = \sum_{j=1}^N c_j F_j(s_+, s_-), \quad \bar{\mathcal{A}} = \sum_{j=1}^N \bar{c}_j \bar{F}_j(s_+, s_-), \quad (2)$$

where F_j and \bar{F}_j are the DP spin-dependent dynamical functions for the resonance, while j and c_j are complex coefficients that account for the relative magnitudes and phases of the N intermediate (resonant and nonresonant) components. The spin-dependent functions $F_j(s_+, s_-)$, embedding the resonance line shape and the angular distributions, are constructed in the Zemach tensor formalism [26]. The weak-phase dependence is included in the c_j coefficients. The results obtained for each isobar amplitude are expressed in this paper as a magnitude and a phase. The magnitude includes any potential B -meson production and experimental asymmetries.

The analysis method consists of a simultaneous DP fit to the six data subsamples defined above, with the shared isobar parameters determined using an unbinned maximum likelihood fit. The DP model is built starting from the most significant amplitudes as determined in previous studies [17–20]. An algorithm to select the relevant additional amplitudes is defined before examining the data. A resonant amplitude is retained in the DP model if at least one of the following requirements is met: (1) a goodness-of-fit estimator based on the point-to-point dissimilarity test [27] decreases when the component is removed from the fit, (2) the likelihood ratio of the two hypotheses (component in and out) decreases, or (3) the precision on the magnitude of the component must be better than 33%, neglecting systematic uncertainties. In particular, the components of the isobar DP model, $f_0(1500)K_S^0$ and $K^*(1680)^-\pi^+$, which were not considered in previous studies, meet all three criteria. By contrast, the amplitude $f_2(1270)K_S^0$ is not retained.

The signal DP model PDF is built from the coherent sum of the amplitudes listed in Table I, normalizing each isobar coefficient to the $K^*(892)^+\pi^-$ reference amplitude. The choice of the $K^*(892)^\pm\pi^\mp$ amplitudes as a reference provides the most stable DP fit. The phases of the reference amplitude and its conjugate are fixed to zero, and the magnitude of the reference amplitude is arbitrarily fixed at 2.

Two dominant backgrounds contaminate the $\bar{B}^0 \rightarrow K_S^0\pi^+\pi^-$ candidate samples: a combinatorial background and a cross-feed background from the decay $\bar{B}_s^0 \rightarrow K_S^0K^\pm\pi^\mp$. The fractions of these backgrounds are measured from the invariant-mass fits performed in Ref. [21], and their DP distributions are determined from the data. The combinatorial background DP model is built from the DP histogram of the $\bar{B}^0 \rightarrow K_S^0\pi^+\pi^-$ candidates with an invariant mass in the range [5450, 5800] MeV/ c^2 . The DP model of the cross-feed background is measured from $\bar{B}_s^0 \rightarrow K_S^0K^\pm\pi^\mp$ candidates, where the K^\pm is reconstructed under the π^\pm hypothesis [21]. The signal fraction depends on the reconstruction category; it is determined from the fit to the invariant-mass distribution and ranges from 85% (Downstream) to 95% (Long). The PDF in Eq. (1) is modified to account for the background components and the signal reconstruction efficiency across the DP, as determined from simulated events.

Two additional observables are formed from the isobar complex coefficients and are measured in the simultaneous DP fit. The asymmetry observables \mathcal{A}_{raw} are derived from the measured isobar parameters of an amplitude j , c_j and \bar{c}_j

$$\mathcal{A}_{\text{raw}} = \frac{|\bar{c}_j|^2 - |c_j|^2}{|\bar{c}_j|^2 + |c_j|^2}. \quad (3)$$

These observables are directly measured for flavor-specific final states. By contrast, the asymmetry of the mode $\bar{B}^0 \rightarrow f_0(980)K_S^0$ is determined using the patterns of its

TABLE I. Components of the DP model used in the fit. The individual amplitudes are referred to by the resonance they contain. The parameter values are given in MeV/ c^2 for the masses and MeV for the widths, except for $f_0(980)$ resonance. The parameter m_0 is the pole mass of the resonance and Γ_0 its natural width. The mass-dependent line shapes employed to model the resonances are indicated in the third column. Relativistic Breit-Wigner and Gounaris-Sakurai line shapes are denoted RBW and GS, respectively. EFKLLM is a parametrization of the $K_S^0\pi^-$ S -wave line shape, $(K\pi)_0^-$.

Resonance	Parameters	Line shape	Value references
$K^*(892)^-$	$m_0 = 891.66 \pm 0.26$ $\Gamma_0 = 50.8 \pm 0.9$	RBW	[28]
$(K\pi)_0^-$	$\mathcal{R}e(\lambda_0) = 0.204 \pm 0.103$ $\mathcal{I}m(\lambda_0) = 0$ $\mathcal{R}e(\lambda_1) = 1$ $\mathcal{I}m(\lambda_1) = 0$	EFKLLM	[29]
$K_2^*(1430)^-$	$m_0 = 1425.6 \pm 1.5$ $\Gamma_0 = 98.5 \pm 2.7$	RBW	[28]
$K^*(1680)^-$	$m_0 = 1717 \pm 27$ $\Gamma_0 = 332 \pm 110$	Flatté [30]	[28]
$f_0(500)$	$m_0 = 513 \pm 32$ $\Gamma_0 = 335 \pm 67$	RBW	[31]
$\rho(770)^0$	$m_0 = 775.26 \pm 0.25$ $\Gamma_0 = 149.8 \pm 0.8$	GS [32]	[28]
$f_0(980)$	$m_0 = 965 \pm 10$ $g_\pi = 0.165 \pm 0.025$ GeV $g_K = 0.695 \pm 0.119$ GeV	Flatté	[33]
$f_0(1500)$	$m_0 = 1505 \pm 6$ $\Gamma_0 = 109 \pm 7$	RBW	[28]
χ_{c0}	$m_0 = 3414.75 \pm 0.31$ $\Gamma_0 = 10.5 \pm 0.6$	RBW	[28]
Nonresonant (NR)		Phase space	

interference with flavor-specific amplitudes. The CP asymmetry is related to the raw asymmetry by $\mathcal{A}_{CP} = \mathcal{A}_{\text{raw}} - \mathcal{A}_\Delta$. The correction asymmetry is defined at first order as $\mathcal{A}_\Delta = A_P(B^0) + A_D(\pi)$, where $A_P(B^0)$ is the production asymmetry between the B^0 and \bar{B}^0 mesons and $A_D(\pi)$ is the detection asymmetry between π^+ and π^- mesons. The production asymmetry $A_P(B^0)$ has been determined to be $A_P(B^0) = (-0.35 \pm 0.81)\%$ [34]. Using D_s^+ decay modes [35], the pion detection asymmetry is measured to be consistent with zero, with a 0.25% uncertainty. The difference in the nuclear cross sections for K^0 and \bar{K}^0 interactions in material results in a negligible bias [36]. The uncertainty due to the correction asymmetries and the experimental systematic uncertainty are added in quadrature.

The rate of a single process is proportional to the square of the relevant matrix element [see Eq. (1)]. This involves the ensemble of its interferences with other components.

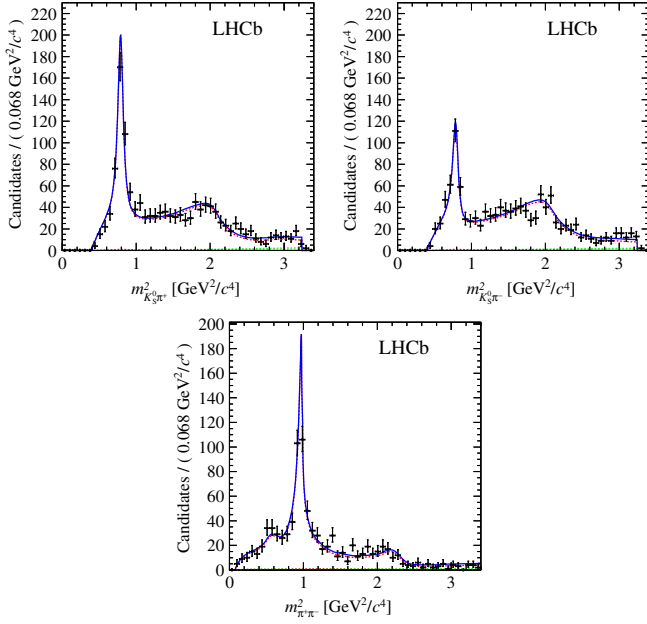


FIG. 2. Projections of the sum of all data categories (black points) and the nominal fit function onto the DP variables (left) $m_{K_S^0\pi^+}^2$, (right) $m_{K_S^0\pi^-}^2$ and (bottom) $m_{\pi^+\pi^-}^2$, restricted to the two-body, low invariant-mass regions. The full fit is shown by the solid blue line and the signal model by the dashed red line. The observed difference is due to the (green) combinatorial and (light red) cross-feed background contributions, barely visible in these projections.

It is convenient to define the CP -averaged fit fraction of the process i , $\mathcal{F}_{(CP)}(i)$, as

$$\mathcal{F}_{(CP)}(i) = \frac{\iint_{\text{DP}} (|c_i F_i(s_+, s_-)|^2 + |\bar{c}_i \bar{F}_i(s_+, s_-)|^2) ds_+ ds_-}{\iint_{\text{DP}} (|\sum_j c_j F_j(s_+, s_-)|^2 + |\sum_j \bar{c}_j \bar{F}_j(s_+, s_-)|^2) ds_+ ds_-}. \quad (4)$$

Simulation is used to determine the selection efficiency of the signal. The simulation does not perfectly reproduce the detector response, and these imperfections are corrected for in several respects. First, the particle identification and misidentification efficiencies are determined from a calibration sample using reconstructed $D^{*+} \rightarrow D^0\pi^+$ decays, where the D^0 meson decays to the Cabibbo-favored $K^-\pi^+$ final state. The variation of the PID performance with the track kinematics is included in the procedure. The calibration is performed using samples from the same data-taking period, accounting for the variation in the performance of the hadron identification detectors over time. Second, inaccuracies of the tracking simulation are mitigated by a weighting of the simulated tracking efficiency to match that which was measured in a calibration sample [37]. Analogous corrections are applied to the K_S^0 decay-

products tracking and vertexing efficiencies. Finally, a control sample of $D^{*+} \rightarrow D^0(\rightarrow K^-\pi^+)\pi^+$ decays is used to quantify the differences of the hardware trigger response in data and simulation for pions and kaons, separated by positive and negative hadron charges, as a function of their transverse momentum [21,38]. The uncertainties assigned to these corrections are taken as a source of systematic uncertainties.

Two categories of systematic uncertainties are considered: experimental and related to the DP model. The former category comprises the uncertainties on the fraction of signal, the fit biases, the variation of the signal efficiency across the DP (including the choice of the efficiency binning), and the background DP models. The DP model uncertainties arise from the limited knowledge of the fixed parameters of the resonance line shape models, the marginal components neglected in the amplitude fit model, and the modeling of the $K_S^0\pi^-$ and $\pi^+\pi^-$ S -wave components.

All of the experimental uncertainties are estimated by means of pseudoexperiments, in which samples for each reconstruction category are simulated and fitted exactly as for the data sample. For each pseudoexperiment, a single parameter governing a systematic effect (e.g., the signal fraction) is varied according to its uncertainty. The standard deviation of the distribution of the fit results in an ensemble of 500 pseudoexperiments is taken as the corresponding systematic error estimate. The largest absolute bias of an individual source of uncertainty is observed at the few percent level. The final result is corrected for any observed bias where it is significant. The dominant contribution to the experimental uncertainty is the efficiency determination.

The mass and the width of each resonance given in Table I are varied individually and symmetrically by one standard deviation to evaluate the impact of the fixed parameters of the isobar resonance line shapes. The Blatt-Weisskopf radius parameter, fixed at 4 GeV^{-1} , is varied by $\pm 1 \text{ GeV}^{-1}$ [18].

To evaluate the systematic uncertainties related to the marginal components of the DP model, the effect of adding the resonance $f_2(1270)$ (which is not retained by the previous criteria) and removing of the $f_0(500)$ component (the least significant contribution in the nominal model) is considered by repeating the fit with and without these components. Based upon this new model, a pseudoexperiment with a signal yield much larger than that of the data is then generated and fit back with the nominal model. The related systematic uncertainty estimate is taken as the difference between the generated and fitted values.

A critical part of the isobar model design is the description of $K_S^0\pi^\pm$ S -wave components. Two parametrizations of these contributions have been studied: LASS [39] and EFKLLM [29]. The latter provides the best fit to the data. The log-likelihood difference between the two model hypotheses is $-2\Delta \ln \mathcal{L} = 85$, which indicates that the LASS parametrization cannot be used to assign a

meaningful systematic uncertainty related to the choice of the model. In absence of a competitive alternative model (to our knowledge), no systematic uncertainty is assigned to the choice of the EFKLLM parametrization. All model uncertainties are combined in quadrature to form the total model of systematic uncertainty.

The Dalitz plot projections are shown in Fig. 2, with the result of the fit superimposed [40]. The CP -averaged fit fractions related to the quasi-two-body and nonresonant amplitudes are determined to be

$$\begin{aligned}\mathcal{F}_{\langle CP \rangle}(K^*(892)^-\pi^+) &= 9.43 \pm 0.40 \pm 0.33 \pm 0.34\%, \\ \mathcal{F}_{\langle CP \rangle}((K\pi)_0^-\pi^+) &= 32.7 \pm 1.4 \pm 1.5 \pm 1.1\%, \\ \mathcal{F}_{\langle CP \rangle}(K_2^*(1430)^-\pi^+) &= 2.45 \pm_{0.08}^{0.10} \pm 0.14 \pm 0.12\%, \\ \mathcal{F}_{\langle CP \rangle}(K^*(1680)^-\pi^+) &= 7.34 \pm 0.30 \pm 0.31 \pm 0.06\%, \\ \mathcal{F}_{\langle CP \rangle}(f_0(980)K_S^0) &= 18.6 \pm 0.8 \pm 0.7 \pm 1.2\%, \\ \mathcal{F}_{\langle CP \rangle}(\rho(770)^0K_S^0) &= 3.8 \pm_{1.6}^{1.1} \pm 0.7 \pm 0.4\%, \\ \mathcal{F}_{\langle CP \rangle}(f_0(500)K_S^0) &= 0.32 \pm_{0.08}^{0.40} \pm 0.19 \pm 0.23\%, \\ \mathcal{F}_{\langle CP \rangle}(f_0(1500)K_S^0) &= 2.60 \pm 0.54 \pm 1.28 \pm 0.60\%, \\ \mathcal{F}_{\langle CP \rangle}(\chi_{c0}K_S^0) &= 2.23 \pm_{0.32}^{0.40} \pm 0.22 \pm 0.13\%, \\ \mathcal{F}_{\langle CP \rangle}(K_S^0\pi^+\pi^-)^{\text{NR}} &= 24.3 \pm 1.3 \pm 3.7 \pm 4.5\%,\end{aligned}$$

where the statistical, experimental systematic and model uncertainties are split accordingly in that order. The results are in agreement with the measurements obtained by the *BABAR* and Belle Collaborations with decay-time-dependent flavor-tagged analyses [17,18], insofar as the DP model components can be compared.

The measurements of the CP asymmetries are

$$\begin{aligned}\mathcal{A}_{CP}(K^*(892)^-\pi^+) &= -0.308 \pm 0.060 \pm 0.011 \pm 0.012, \\ \mathcal{A}_{CP}((K\pi)_0^-\pi^+) &= -0.032 \pm 0.047 \pm 0.016 \pm 0.027, \\ \mathcal{A}_{CP}(K_2^*(1430)^-\pi^+) &= -0.29 \pm 0.22 \pm 0.09 \pm 0.03, \\ \mathcal{A}_{CP}(K^*(1680)^-\pi^+) &= -0.07 \pm 0.13 \pm 0.02 \pm 0.03, \\ \mathcal{A}_{CP}(f_0(980)K_S^0) &= 0.28 \pm 0.27 \pm 0.05 \pm 0.14,\end{aligned}$$

where the uncertainties are statistical, experimental systematic and from the model. The statistical significance of having observed a nonvanishing CP asymmetry in the decay $\bar{B}^0 \rightarrow K^*(892)^-\pi^+$, built from the likelihood ratio for the null hypothesis, is 6.7 standard deviations and reduces to about 6 standard deviations, taking into account the systematic uncertainties. This measurement constitutes the first observation of a CP -violating asymmetry in the decay $\bar{B}^0 \rightarrow K^*(892)^-\pi^+$. The measured value is in good agreement with the world average $\mathcal{A}_{CP}(K^*(892)^-\pi^+) = -0.23 \pm 0.06$ [4] with a similar precision. It is also consistent with SM predictions using

different QCD-inspired approaches to handle the hadronic matrix elements of the decays [41–43]. This measurement can also be used with other experimental inputs and theoretical assumptions to set nontrivial constraints on the Cabibbo-Kobayashi-Maskawa parameters [44].

We express our gratitude to our colleagues in the CERN accelerator departments for the excellent performance of the LHC. We thank the technical and administrative staff at the LHCb institutes. We acknowledge support from CERN and from the national agencies: CAPES, CNPq, FAPERJ, and FINEP (Brazil); MOST and NSFC (China); CNRS/IN2P3 (France); BMBF, DFG, and MPG (Germany); INFN (Italy); NWO (The Netherlands); MNiSW and NCN (Poland); MEN/IFA (Romania); MinES and FASO (Russia); MinECo (Spain); SNSF and SER (Switzerland); NASU (Ukraine); STFC (United Kingdom); NSF (USA). We acknowledge the computing resources that are provided by CERN, IN2P3 (France), KIT and DESY (Germany), INFN (Italy), SURF (The Netherlands), PIC (Spain), GridPP (United Kingdom), RRCKI and Yandex LLC (Russia), CSCS (Switzerland), IFIN-HH (Romania), CBPF (Brazil), PL-GRID (Poland), and OSC (USA). We are indebted to the communities behind the multiple open-source software packages on which we depend. Individual groups or members have received support from AvH Foundation (Germany), EPLANET, Marie Skłodowska-Curie Actions and ERC (European Union), ANR, Labex P2IO, ENIGMASS and OCEVU, and Région Auvergne-Rhône-Alpes (France), RFBR and Yandex LLC (Russia), GVA, XuntaGal and GENCAT (Spain), Herchel Smith Fund, the Royal Society, the English-Speaking Union, and the Leverhulme Trust (United Kingdom).

-
- [1] J. H. Christenson, J. W. Cronin, V. L. Fitch, and R. Turlay, Evidence for the 2π Decay of the K_2^0 Meson, *Phys. Rev. Lett.* **13**, 138 (1964).
 - [2] B. Aubert *et al.* (*BABAR* Collaboration), Observation of CP Violation in the B^0 Meson System, *Phys. Rev. Lett.* **87**, 091801 (2001).
 - [3] K. Abe *et al.* (Belle Collaboration), Observation of Large CP Violation in the Neutral B Meson System, *Phys. Rev. Lett.* **87**, 091802 (2001).
 - [4] Y. Amhis *et al.* (Heavy Flavor Averaging Group), Averages of b -hadron, c -hadron, and τ -lepton properties as of summer 2016, *Eur. Phys. J. C* **77**, 895 (2017).
 - [5] M. Beneke and M. Neubert, QCD factorization for $B \rightarrow PP$ and $B \rightarrow PV$ decays, *Nucl. Phys.* **B675**, 333 (2003).
 - [6] R. Fleischer, S. Recksiegel, and F. Schwab, On puzzles and non-puzzles in $B \rightarrow \pi\pi$, πK decays, *Eur. Phys. J. C* **51**, 55 (2007).
 - [7] S. Baek, C.-W. Chiang, and D. London, The $B \rightarrow \pi K$ puzzle: 2009 update, *Phys. Lett. B* **675**, 59 (2009).
 - [8] H.-n. Li and S. Mishima, Possible resolution of the $B \rightarrow \pi\pi$, πK puzzles, *Phys. Rev. D* **83**, 034023 (2011).

- [9] S. Khalil, A. Masiero, and H. Murayama, $B \rightarrow K\pi$ puzzle and new sources of CP violation in supersymmetry, *Phys. Lett. B* **682**, 74 (2009).
- [10] N. Cabibbo, Unitary Symmetry and Leptonic Decays, *Phys. Rev. Lett.* **10**, 531 (1963).
- [11] M. Kobayashi and T. Maskawa, CP violation in the renormalizable theory of weak interaction, *Prog. Theor. Phys.* **49**, 652 (1973).
- [12] G. Buchalla, G. Hiller, Y. Nir, and G. Raz, The pattern of CP asymmetries in $b \rightarrow s$ transitions, *J. High Energy Phys.* **09** (2005) 074.
- [13] Y. Grossman and M. P. Worah, CP asymmetries in B decays with new physics in decay amplitudes, *Phys. Lett. B* **395**, 241 (1997).
- [14] D. London and A. Soni, Measuring the CP angle β in hadronic $b \rightarrow s$ penguin decays, *Phys. Lett. B* **407**, 61 (1997).
- [15] M. Ciuchini, E. Franco, G. Martinelli, A. Masiero, and L. Silvestrini, CP Violating B Decays in the Standard Model and Supersymmetry, *Phys. Rev. Lett.* **79**, 978 (1997).
- [16] R. H. Dalitz, On the analysis of tau-meson data and the nature of the tau-meson, *Philos. Mag.* **44**, 1068 (1953).
- [17] J. Dalseno *et al.* (Belle Collaboration), Time-dependent Dalitz Plot measurement of CP parameters in $B^0 \rightarrow K_S^0 \pi^+ \pi^-$ decays, *Phys. Rev. D* **79**, 072004 (2009).
- [18] B. Aubert *et al.* (BABAR Collaboration), Time-dependent amplitude analysis of $B^0 \rightarrow K_S^0 \pi^+ \pi^-$, *Phys. Rev. D* **80**, 112001 (2009).
- [19] Y. Nakahama *et al.* (Belle Collaboration), Measurement of CP violating asymmetries in $B^0 \rightarrow K_S^0 K^+ K^-$ decays with a time-dependent Dalitz approach, *Phys. Rev. D* **82**, 073011 (2010).
- [20] J. P. Lees *et al.* (BABAR Collaboration), Study of CP violation in Dalitz-plot analyses of $B^0 \rightarrow K^+ K^- K_S^0$, $B^+ \rightarrow K^+ K^- K^+$, and $B^+ \rightarrow K_S^0 K_S^0 K^+$, *Phys. Rev. D* **85**, 112010 (2012).
- [21] R. Aaij *et al.* (LHCb Collaboration), Updated branching fraction measurements of $B_{(s)}^0 \rightarrow K_S^0 h^+ h^-$ decays, *J. High Energy Phys.* **11** (2017) 027.
- [22] A. A. Alves Jr. *et al.* (LHCb Collaboration), The LHCb detector at the LHC, *J. Instrum.* **3**, S08005 (2008).
- [23] R. Aaij *et al.* (LHCb Collaboration), LHCb detector performance, *Int. J. Mod. Phys. A* **30**, 1530022 (2015).
- [24] V. V. Gligorov and M. Williams, Efficient, reliable and fast high-level triggering using a bonsai boosted decision tree, *J. Instrum.* **8**, P02013 (2013).
- [25] I. Bigi and A. Sanda, CP Violation, *Monographs on Particle Physics, Nuclear Physics and Cosmology* (Cambridge University Press, Cambridge, UK, 2000), DOI: 10.1017/CBO9780511581014.
- [26] C. Zemach, Determination of the spins and parities of resonances, *Phys. Rev.* **140**, B109 (1965).
- [27] M. Williams, How good are your fits? Unbinned multivariate goodness-of-fit tests in high energy physics, *J. Instrum.* **5**, P09004 (2010).
- [28] C. Patrignani *et al.* (Particle Data Group), Review of particle physics, *Chin. Phys. C* **40**, 100001 (2016).
- [29] B. El-Bennich, A. Furman, R. Kaminski, L. Lesniak, B. Loiseau, and B. Moussallam, CP violation and kaon-pion interactions in $B \rightarrow K\pi^+\pi^-$ decays, *Phys. Rev. D* **79**, 094005 (2009); Erratum, *Phys. Rev. D* **83**, 039903 (2011).
- [30] S. M. Flatté, Coupled-channel analysis of the $\pi\eta$ and $K\bar{K}$ systems near $K\bar{K}$ threshold, *Phys. Lett. B* **63**, 224 (1976).
- [31] H. Muramatsu *et al.* (CLEO Collaboration), Dalitz Analysis of $D^0 \rightarrow K_S^0 \pi^+ \pi^-$, *Phys. Rev. Lett.* **89** (2002) 251802.
- [32] G. J. Gounaris and J. J. Sakurai, Finite-Width Corrections to the Vector-Meson Dominance Prediction for $\rho \rightarrow e^+ e^-$, *Phys. Rev. Lett.* **21**, 244 (1968).
- [33] M. Ablikim *et al.* (BES Collaboration), Resonances in $J/\psi \rightarrow \phi\pi^+\pi^-$ and $\phi K^+ K^-$, *Phys. Lett. B* **607**, 243 (2005).
- [34] R. Aaij *et al.* (LHCb Collaboration), First Observation of CP Violation in the Decays of B_s^0 Mesons, *Phys. Rev. Lett.* **110**, 221601 (2013).
- [35] R. Aaij *et al.* (LHCb Collaboration), Measurement of the $D_s^+ D_s^-$ production asymmetry in 7 MeV pp collisions, *Phys. Lett. B* **713**, 186 (2012).
- [36] B. R. Ko, E. Won, B. Golob, and P. Pakhlov, Effect of nuclear interactions of neutral kaons on CP asymmetry measurements, *Phys. Rev. D* **84**, 111501 (2011).
- [37] M. De Cian *et al.*, Measurement of the track finding efficiency, CERN Report No. LHCb-PUB-2011-025.
- [38] R. Aaij *et al.*, The LHCb trigger and its performance in 2011, *J. Instrum.* **8**, P04022 (2013).
- [39] D. Aston *et al.*, A study of $K^- \pi^+$ scattering in the reaction $K^- p \rightarrow K^- \pi^+ n$ at 11 GeV/c, *Nucl. Phys.* **B296**, 493 (1988).
- [40] See Supplemental Material at <http://link.aps.org/supplemental/10.1103/PhysRevLett.120.261801>, for the two-dimensional projection of the DP model.
- [41] Q. Chang, X.-Q. Li, and Y.-D. Yang, Revisiting $B \rightarrow \pi K$, πK^* and ρK decays: Direct CP violation and implication for new physics, *J. High Energy Phys.* **09** (2008) 038.
- [42] W. Wang, Y.-M. Wang, D.-S. Yang, and C.-D. Lu, Charmless two-body $B_{(s)} \rightarrow VP$ decays in soft collinear effective theory, *Phys. Rev. D* **78**, 034011 (2008).
- [43] H.-Y. Cheng, C.-W. Chiang, and A.-L. Kuo, Updating $B \rightarrow PP$, VP decays in the framework of flavor symmetry, *Phys. Rev. D* **91**, 014011 (2015).
- [44] J. Charles, S. Descotes-Genon, J. Ocariz, and A. Pérez Pérez, Disentangling weak and strong interactions in $B \rightarrow K^*(\rightarrow K\pi)\pi$ Dalitz-plot analyses, *Eur. Phys. J. C* **77**, 561 (2017).

R. Aaij,⁴⁰ B. Adeva,³⁹ M. Adinolfi,⁴⁸ Z. Ajaltouni,⁵ S. Akar,⁵⁹ J. Albrecht,¹⁰ F. Alessio,⁴⁰ M. Alexander,⁵³ A. Alfonso Alberro,³⁸ S. Ali,⁴³ G. Alkhazov,³¹ P. Alvarez Cartelle,⁵⁵ A. A. Alves Jr.,⁵⁹ S. Amato,² S. Amerio,²³ Y. Amhis,⁷ L. An,³ L. Anderlini,¹⁸ G. Andreassi,⁴¹ M. Andreotti,^{17,g} J. E. Andrews,⁶⁰ R. B. Appleby,⁵⁶ F. Archilli,⁴³ P. d'Argent,¹²

J. Arnau Romeu,⁶ A. Artamonov,³⁷ M. Artuso,⁶¹ E. Aslanides,⁶ M. Atzeni,⁴² G. Auriemma,²⁶ M. Baalouch,⁵ I. Babuschkin,⁵⁶ S. Bachmann,¹² J. J. Back,⁵⁰ A. Badalov,^{38,m} C. Baesso,⁶² S. Baker,⁵⁵ V. Balagura,^{7,b} W. Baldini,¹⁷ A. Baranov,³⁵ R. J. Barlow,⁵⁶ C. Barschel,⁴⁰ S. Barsuk,⁷ W. Barter,⁵⁶ F. Baryshnikov,³² V. Batozskaya,²⁹ V. Battista,⁴¹ A. Bay,⁴¹ L. Beaucourt,⁴ J. Beddow,⁵³ F. Bedeschi,²⁴ I. Bediaga,¹ A. Beiter,⁶¹ L. J. Bel,⁴³ N. Belyi,⁶³ V. Bellee,⁴¹ N. Belloli,^{21,i} K. Belous,³⁷ I. Belyaev,^{32,40} E. Ben-Haim,⁸ G. Bencivenni,¹⁹ S. Benson,⁴³ S. Beranek,⁹ A. Berezhnoy,³³ R. Bernet,⁴² D. Berninghoff,¹² E. Bertholet,⁸ A. Bertolin,²³ C. Betancourt,⁴² F. Betti,¹⁵ M.-O. Bettler,⁴⁰ M. van Beuzekom,⁴³ Ia. Bezshyiko,⁴² S. Bifani,⁴⁷ P. Billoir,⁸ A. Birnkraut,¹⁰ A. Bizzeti,^{18,u} M. Bjørn,⁵⁷ T. Blake,⁵⁰ F. Blanc,⁴¹ S. Blusk,⁶¹ V. Bocci,²⁶ T. Boettcher,⁵⁸ A. Bondar,^{36,w} N. Bondar,³¹ I. Bordyuzhin,³² S. Borghi,⁵⁶ M. Borisyak,³⁵ M. Borsato,³⁹ F. Bossu,⁷ M. Boudir,⁹ T. J. V. Bowcock,⁵⁴ E. Bowen,⁴² C. Bozzi,^{17,40} S. Braun,¹² T. Britton,⁶¹ J. Brodzicka,²⁷ D. Brundu,¹⁶ E. Buchanan,⁴⁸ C. Burr,⁵⁶ A. Bursche,^{16,f} J. Buytaert,⁴⁰ W. Byczynski,⁴⁰ S. Cadeddu,¹⁶ H. Cai,⁶⁴ R. Calabrese,^{17,g} R. Calladine,⁴⁷ M. Calvi,^{21,i} M. Calvo Gomez,^{38,m} A. Camboni,^{38,m} P. Campana,¹⁹ D. H. Campora Perez,⁴⁰ L. Capriotti,⁵⁶ A. Carbone,^{15,e} G. Carboni,^{25,j} R. Cardinale,^{20,h} A. Cardini,¹⁶ P. Carniti,^{21,i} L. Carson,⁵² K. Carvalho Akiba,² G. Casse,⁵⁴ L. Cassina,²¹ M. Cattaneo,⁴⁰ G. Cavallero,^{20,40,h} R. Cenci,^{24,t} D. Chamont,⁷ M. Charles,⁸ Ph. Charpentier,⁴⁰ G. Chatzikonstantinidis,⁴⁷ M. Chefdeville,⁴ S. Chen,¹⁶ S. F. Cheung,⁵⁷ S.-G. Chitic,⁴⁰ V. Chobanova,^{39,40} M. Chrzaszcz,^{42,27} A. Chubykin,³¹ P. Ciambone,¹⁹ X. Cid Vidal,³⁹ G. Ciezarek,⁴³ P. E. L. Clarke,⁵² M. Clemencic,⁴⁰ H. V. Cliff,⁴⁹ J. Closier,⁴⁰ J. Cogan,⁶ E. Cogneras,⁵ V. Cogoni,^{16,f} L. Cojocariu,³⁰ P. Collins,⁴⁰ T. Colombo,⁴⁰ A. Comerma-Montells,¹² A. Contu,⁴⁰ A. Cook,⁴⁸ G. Coombs,⁴⁰ S. Coquereau,³⁸ G. Corti,⁴⁰ M. Corvo,^{17,g} C. M. Costa Sobral,⁵⁰ B. Couturier,⁴⁰ G. A. Cowan,⁵² D. C. Craik,⁵⁸ A. Crocombe,⁵⁰ M. Cruz Torres,¹ R. Currie,⁵² C. D'Ambrosio,⁴⁰ F. Da Cunha Marinho,² E. Dall'Occo,⁴³ J. Dalseno,⁴⁸ A. Davis,³ O. De Aguiar Francisco,⁴⁰ S. De Capua,⁵⁶ M. De Cian,¹² J. M. De Miranda,¹ L. De Paula,² M. De Serio,^{14,d} P. De Simone,¹⁹ C. T. Dean,⁵³ D. Decamp,⁴ L. Del Buono,⁸ H.-P. Dembinski,¹¹ M. Demmer,¹⁰ A. Dendek,²⁸ D. Derkach,³⁵ O. Deschamps,⁵ F. Dettori,⁵⁴ B. Dey,⁶⁵ A. Di Canto,⁴⁰ P. Di Nezza,¹⁹ H. Dijkstra,⁴⁰ F. Dordei,⁴⁰ M. Dorigo,⁴⁰ A. Dosil Suárez,³⁹ L. Douglas,⁵³ A. Dovbnya,⁴⁵ K. Dreimanis,⁵⁴ L. Dufour,⁴³ G. Dujany,⁸ P. Durante,⁴⁰ R. Dzhelezhyan,³⁷ M. Dziewiecki,¹² A. Dziurda,⁴⁰ A. Dzyuba,³¹ S. Easo,⁵¹ M. Ebert,⁵² U. Egede,⁵⁵ V. Egorychev,³² S. Eidelman,^{36,w} S. Eisenhardt,⁵² U. Eitschberger,¹⁰ R. Ekelhof,¹⁰ L. Eklund,⁵³ S. Ely,⁶¹ S. Esen,¹² H. M. Evans,⁴⁹ T. Evans,⁵⁷ A. Falabella,¹⁵ N. Farley,⁴⁷ S. Farry,⁵⁴ D. Fazzini,^{21,i} L. Federici,²⁵ D. Ferguson,⁵² G. Fernandez,³⁸ P. Fernandez Declara,⁴⁰ A. Fernandez Prieto,³⁹ F. Ferrari,¹⁵ F. Ferreira Rodrigues,² M. Ferro-Luzzi,⁴⁰ S. Filippov,³⁴ R. A. Fini,¹⁴ M. Fiorini,^{17,g} M. Firlej,²⁸ C. Fitzpatrick,⁴¹ T. Fiutowski,²⁸ F. Fleuret,^{7,b} K. Fohl,⁴⁰ M. Fontana,^{16,40} F. Fontanelli,^{20,h} D. C. Forshaw,⁶¹ R. Forty,⁴⁰ V. Franco Lima,⁵⁴ M. Frank,⁴⁰ C. Frei,⁴⁰ J. Fu,^{22,q} W. Funk,⁴⁰ E. Furfaro,^{25,j} C. Färber,⁴⁰ E. Gabriel,⁵² A. Gallas Torreira,³⁹ D. Galli,^{15,e} S. Gallorini,²³ S. Gambetta,⁵² M. Gandelman,² P. Gandini,²² Y. Gao,³ L. M. Garcia Martin,⁷⁰ J. García Pardiñas,³⁹ J. Garra Tico,⁴⁹ L. Garrido,³⁸ P. J. Garsed,⁴⁹ D. Gascon,³⁸ C. Gaspar,⁴⁰ L. Gavardi,¹⁰ G. Gazzoni,⁵ D. Gerick,¹² E. Gersabeck,⁵⁶ M. Gersabeck,⁵⁶ T. Gershon,⁵⁰ Ph. Ghez,⁴ S. Gianì,⁴¹ V. Gibson,⁴⁹ O. G. Girard,⁴¹ L. Giubega,³⁰ K. Gizdov,⁵² V. V. Gligorov,⁸ D. Golubkov,³² A. Golutvin,⁵⁵ A. Gomes,^{1,a} I. V. Gorelov,³³ C. Gotti,^{21,i} E. Govorkova,⁴³ J. P. Grabowski,¹² R. Graciani Diaz,³⁸ L. A. Granado Cardoso,⁴⁰ E. Graugés,³⁸ E. Graverini,⁴² G. Graziani,¹⁸ A. Grecu,³⁰ R. Greim,⁹ P. Griffith,¹⁶ L. Grillo,²¹ L. Gruber,⁴⁰ B. R. Gruber Cazon,⁵⁷ O. Grünberg,⁶⁷ E. Gushchin,³⁴ Yu. Guz,³⁷ T. Gys,⁴⁰ C. Göbel,⁶² T. Hadavizadeh,⁵⁷ C. Hadjivasiliou,⁵ G. Haefeli,⁴¹ C. Haen,⁴⁰ S. C. Haines,⁴⁹ B. Hamilton,⁶⁰ X. Han,¹² T. H. Hancock,⁵⁷ S. Hansmann-Menzemer,¹² N. Harnew,⁵⁷ S. T. Harnew,⁴⁸ C. Hasse,⁴⁰ M. Hatch,⁴⁰ J. He,⁶³ M. Hecker,⁵⁵ K. Heinicke,¹⁰ A. Heister,⁹ K. Hennessy,⁵⁴ P. Henrard,⁵ L. Henry,⁷⁰ E. van Herwijnen,⁴⁰ M. Heß,⁶⁷ A. Hicheur,² D. Hill,⁵⁷ C. Hombach,⁵⁶ P. H. Hopchev,⁴¹ W. Hu,⁶⁵ Z. C. Huard,⁵⁹ W. Hulsbergen,⁴³ T. Humair,⁵⁵ M. Hushchyn,³⁵ D. Hutchcroft,⁵⁴ P. Ibis,¹⁰ M. Idzik,²⁸ P. Ilten,⁵⁸ R. Jacobsson,⁴⁰ J. Jalocho,⁵⁷ E. Jans,⁴³ A. Jawahery,⁶⁰ F. Jiang,³ M. John,⁵⁷ D. Johnson,⁴⁰ C. R. Jones,⁴⁹ C. Joram,⁴⁰ B. Jost,⁴⁰ N. Jurik,⁵⁷ S. Kandybei,⁴⁵ M. Karacson,⁴⁰ J. M. Kariuki,⁴⁸ S. Karodia,⁵³ N. Kazeev,³⁵ M. Kecke,¹² F. Keizer,⁴⁹ M. Kelsey,⁶¹ M. Kenzie,⁴⁹ T. Ketel,⁴⁴ E. Khairullin,³⁵ B. Khanji,¹² C. Khurewathanakul,⁴¹ T. Kirn,⁹ S. Klaver,⁵⁶ K. Klimaszewski,²⁹ T. Klimkovich,¹¹ S. Kolliiev,⁴⁶ M. Kolpin,¹² R. Kopečna,¹² P. Koppenburg,⁴³ A. Kosmyntseva,³² S. Kotriakhova,³¹ M. Kozeiha,⁵ L. Kravchuk,³⁴ M. Kreps,⁵⁰ F. Kress,⁵⁵ P. Krokovny,^{36,w} F. Kruse,¹⁰ W. Krzemien,²⁹ W. Kucewicz,^{27,l} M. Kucharczyk,²⁷ V. Kudryavtsev,^{36,w} A. K. Kuonen,⁴¹ T. Kvaratskheliya,^{32,40} D. Lacarrere,⁴⁰ G. Lafferty,⁵⁶ A. Lai,¹⁶ G. Lanfranchi,¹⁹ C. Langenbruch,⁹ T. Latham,⁵⁰ C. Lazzaroni,⁴⁷ R. Le Gac,⁶ A. Leflat,^{33,40} J. Lefrançois,⁷ R. Lefèvre,⁵ F. Lemaître,⁴⁰ E. Lemos Cid,³⁹ O. Leroy,⁶ T. Lesiak,²⁷ B. Leverington,¹² P.-R. Li,⁶³ T. Li,³ Y. Li,⁷ Z. Li,⁶¹ T. Likhomanenko,⁶⁸ R. Lindner,⁴⁰ F. Lionetto,⁴² V. Lisovskyi,⁷ X. Liu,³ D. Loh,⁵⁰ A. Loi,¹⁶ I. Longstaff,⁵³ J. H. Lopes,² D. Lucchesi,^{23,o} M. Lucio Martinez,³⁹ H. Luo,⁵² A. Lupato,²³ E. Luppi,^{17,g} O. Lupton,⁴⁰ A. Lusiani,²⁴ X. Lyu,⁶³ F. Machefert,⁷ F. Maciuc,³⁰ V. Macko,⁴¹ P. Mackowiak,¹⁰

S. Maddrell-Mander,⁴⁸ O. Maev,^{31,40} K. Maguire,⁵⁶ D. Maisuzenko,³¹ M. W. Majewski,²⁸ S. Malde,⁵⁷ B. Malecki,²⁷ A. Malinin,⁶⁸ T. Maltsev,^{36,w} G. Manca,^{16,f} G. Mancinelli,⁶ D. Marangotto,^{22,q} J. Maratas,^{5,v} J. F. Marchand,⁴ U. Marconi,¹⁵ C. Marin Benito,³⁸ M. Marinangeli,⁴¹ P. Marino,⁴¹ J. Marks,¹² G. Martellotti,²⁶ M. Martin,⁶ M. Martinelli,⁴¹ D. Martinez Santos,³⁹ F. Martinez Vidal,⁷⁰ L. M. Massacrier,⁷ A. Massafferri,¹ R. Matev,⁴⁰ A. Mathad,⁵⁰ Z. Mathe,⁴⁰ C. Matteuzzi,²¹ A. Mauri,⁴² E. Maurice,^{7,b} B. Maurin,⁴¹ A. Mazurov,⁴⁷ M. McCann,^{55,40} A. McNab,⁵⁶ R. McNulty,¹³ J. V. Mead,⁵⁴ B. Meadows,⁵⁹ C. Meaux,⁶ F. Meier,¹⁰ N. Meinert,⁶⁷ D. Melnychuk,²⁹ M. Merk,⁴³ A. Merli,^{22,40,q} E. Michielin,²³ D. A. Milanes,⁶⁶ E. Millard,⁵⁰ M.-N. Minard,⁴ L. Minzoni,¹⁷ D. S. Mitzel,¹² A. Mogini,⁸ J. Molina Rodriguez,¹ T. Mombacher,¹⁰ I. A. Monroy,⁶⁶ S. Monteil,⁵ M. Morandin,²³ M. J. Morello,^{24,t} O. Morgunova,⁶⁸ J. Moron,²⁸ A. B. Morris,⁵² R. Mountain,⁶¹ F. Muheim,⁵² M. Mulder,⁴³ D. Müller,⁵⁶ J. Müller,¹⁰ K. Müller,⁴² V. Müller,¹⁰ P. Naik,⁴⁸ T. Nakada,⁴¹ R. Nandakumar,⁵¹ A. Nandi,⁵⁷ I. Nasteva,² M. Needham,⁵² N. Neri,^{22,40} S. Neubert,¹² N. Neufeld,⁴⁰ M. Neuner,¹² T. D. Nguyen,⁴¹ C. Nguyen-Mau,^{41,n} S. Nieswand,⁹ R. Niet,¹⁰ N. Nikitin,³³ T. Nikodem,¹² A. Nogay,⁶⁸ D. P. O'Hanlon,⁵⁰ A. Oblakowska-Mucha,²⁸ V. Obraztsov,³⁷ S. Ogilvy,¹⁹ R. Oldeman,^{16,f} C. J. G. Onderwater,⁷¹ A. Ossowska,²⁷ J. M. Otalora Goicochea,² P. Owen,⁴² A. Oyanguren,⁷⁰ P. R. Pais,⁴¹ A. Palano,¹⁴ M. Palutan,^{19,40} A. Papanestis,⁵¹ M. Pappagallo,^{14,d} L. L. Pappalardo,^{17,g} W. Parker,⁶⁰ C. Parkes,⁵⁶ G. Passaleva,^{18,40} A. Pastore,^{14,d} M. Patel,⁵⁵ C. Patrignani,^{15,e} A. Pearce,⁴⁰ A. Pellegrino,⁴³ G. Penso,²⁶ M. Pepe Altarelli,⁴⁰ S. Perazzini,⁴⁰ P. Perret,⁵ L. Pescatore,⁴¹ K. Petridis,⁴⁸ A. Petrolini,^{20,h} A. Petrov,⁶⁸ M. Petruzzo,^{22,q} E. Picatoste Olloqui,³⁸ B. Pietrzyk,⁴ M. Pikies,²⁷ D. Pinci,²⁶ A. Pistone,^{20,h} A. Piucci,¹² V. Placinta,³⁰ S. Playfer,⁵² M. Plo Casasus,³⁹ F. Polci,⁸ M. Poli Lener,¹⁹ A. Poluektov,⁵⁰ I. Polyakov,⁶¹ E. Polycarpo,² G. J. Pomery,⁴⁸ S. Ponce,⁴⁰ A. Popov,³⁷ D. Popov,^{11,40} S. Poslavskii,³⁷ C. Potterat,² E. Price,⁴⁸ J. Prisciandaro,³⁹ C. Prouve,⁴⁸ V. Pugatch,⁴⁶ A. Puig Navarro,⁴² H. Pullen,⁵⁷ G. Punzi,^{24,p} W. Qian,⁵⁰ R. Quagliani,^{7,48} B. Quintana,⁵ B. Rachwal,²⁸ J. H. Rademacker,⁴⁸ M. Rama,²⁴ M. Ramos Pernas,³⁹ M. S. Rangel,² I. Raniuk,^{45,†} F. Ratnikov,³⁵ G. Raven,⁴⁴ M. Ravonel Salzgeber,⁴⁰ M. Reboud,⁴ F. Redi,⁵⁵ S. Reichert,¹⁰ A. C. dos Reis,¹ C. Remon Alepuz,⁷⁰ V. Renaudin,⁷ S. Ricciardi,⁵¹ S. Richards,⁴⁸ M. Rihl,⁴⁰ K. Rinnert,⁵⁴ V. Rives Molina,³⁸ P. Robbe,⁷ A. Robert,⁸ A. B. Rodrigues,¹ E. Rodrigues,⁵⁹ J. A. Rodriguez Lopez,⁶⁶ A. Rogozhnikov,³⁵ S. Roiser,⁴⁰ A. Rollings,⁵⁷ V. Romanovskiy,³⁷ A. Romero Vidal,³⁹ J. W. Ronayne,¹³ M. Rotondo,¹⁹ M. S. Rudolph,⁶¹ T. Ruf,⁴⁰ P. Ruiz Valls,⁷⁰ J. Ruiz Vidal,⁷⁰ J. J. Saborido Silva,³⁹ E. Sadykhov,³² N. Sagidova,³¹ B. Saitta,^{16,f} V. Salustino Guimaraes,¹ C. Sanchez Mayordomo,⁷⁰ B. Sanmartin Sedes,³⁹ R. Santacesaria,²⁶ C. Santamarina Rios,³⁹ M. Santimaria,¹⁹ E. Santovetti,^{25,j} G. Sarpis,⁵⁶ A. Sarti,^{19,k} C. Satriano,^{26,s} A. Satta,²⁵ D. M. Saunders,⁴⁸ D. Savrina,^{32,33} S. Schael,⁹ M. Schellenberg,¹⁰ M. Schiller,⁵³ H. Schindler,⁴⁰ M. Schmelling,¹¹ T. Schmelzer,¹⁰ B. Schmidt,⁴⁰ O. Schneider,⁴¹ A. Schopper,⁴⁰ H. F. Schreiner,⁵⁹ M. Schubiger,⁴¹ M.-H. Schune,⁷ R. Schwemmer,⁴⁰ B. Sciascia,¹⁹ A. Sciubba,^{26,k} A. Semennikov,³² E. S. Sepulveda,⁸ A. Sergi,⁴⁷ N. Serra,⁴² J. Serrano,⁶ L. Sestini,²³ P. Seyfert,⁴⁰ M. Shapkin,³⁷ I. Shapoval,⁴⁵ Y. Shcheglov,³¹ T. Shears,⁵⁴ L. Shekhtman,^{36,w} V. Shevchenko,⁶⁸ B. G. Siddi,¹⁷ R. Silva Coutinho,⁴² L. Silva de Oliveira,² G. Simi,^{23,o} S. Simone,^{14,d} M. Sirendi,⁴⁹ N. Skidmore,⁴⁸ T. Skwarnicki,⁶¹ E. Smith,⁵⁵ I. T. Smith,⁵² J. Smith,⁴⁹ M. Smith,⁵⁵ I. Soares Lavoura,¹ M. D. Sokoloff,⁵⁹ F. J. P. Soler,⁵³ B. Souza De Paula,² B. Spaan,¹⁰ P. Spradlin,⁵³ S. Sridharan,⁴⁰ F. Stagni,⁴⁰ M. Stahl,¹² S. Stahl,⁴⁰ P. Stefko,⁴¹ S. Stefkova,⁵⁵ O. Steinkamp,⁴² S. Stemmler,¹² O. Stenyakin,³⁷ M. Stepanova,³¹ H. Stevens,¹⁰ S. Stone,⁶¹ B. Storaci,⁴² S. Stracka,^{24,p} M. E. Stramaglia,⁴¹ M. Straticiu,³⁰ U. Straumann,⁴² J. Sun,³ L. Sun,⁶⁴ W. Sutcliffe,⁵⁵ K. Swientek,²⁸ V. Syropoulos,⁴⁴ T. Szumlak,²⁸ M. Szymanski,⁶³ S. T'Jampens,⁴ A. Tayduganov,⁶ T. Tekampe,¹⁰ G. Tellarini,^{17,g} F. Teubert,⁴⁰ E. Thomas,⁴⁰ J. van Tilburg,⁴³ M. J. Tilley,⁵⁵ V. Tisserand,⁴ M. Tobin,⁴¹ S. Tolk,⁴⁹ L. Tomassetti,^{17,g} D. Tonelli,²⁴ F. Toriello,⁶¹ R. Tourinho Jadallah Aoude,¹ E. Tournefier,⁴ M. Traill,⁵³ M. T. Tran,⁴¹ M. Tresch,⁴² A. Trisovic,⁴⁰ A. Tsaregorodtsev,⁶ P. Tsopelas,⁴³ A. Tully,⁴⁹ N. Tuning,^{43,40} A. Ukleja,²⁹ A. Usachov,⁷ A. Ustyuzhanin,³⁵ U. Uwer,¹² C. Vacca,^{16,f} A. Vagner,⁶⁹ V. Vagnoni,^{15,40} A. Valassi,⁴⁰ S. Valat,⁴⁰ G. Valenti,¹⁵ R. Vazquez Gomez,⁴⁰ P. Vazquez Regueiro,³⁹ S. Vecchi,¹⁷ M. van Veghel,⁴³ J. J. Velthuis,⁴⁸ M. Veltri,^{18,r} G. Veneziano,⁵⁷ A. Venkateswaran,⁶¹ T. A. Verlage,⁹ M. Vernet,⁵ M. Vesterinen,⁵⁷ J. V. Viana Barbosa,⁴⁰ B. Viaud,⁷ D. Vieira,⁶³ M. Vieites Diaz,³⁹ H. Viemann,⁶⁷ X. Vilasis-Cardona,^{38,m} M. Vitti,⁴⁹ V. Volkov,³³ A. Vollhardt,⁴² B. Voneki,⁴⁰ A. Vorobyev,³¹ V. Vorobyev,^{36,w} C. Voß,⁹ J. A. de Vries,⁴³ C. Vázquez Sierra,³⁹ R. Waldi,⁶⁷ C. Wallace,⁵⁰ R. Wallace,¹³ J. Walsh,²⁴ J. Wang,⁶¹ D. R. Ward,⁴⁹ H. M. Wark,⁵⁴ N. K. Watson,⁴⁷ D. Websdale,⁵⁵ A. Weiden,⁴² C. Weisser,⁵⁸ M. Whitehead,⁴⁰ J. Wicht,⁵⁰ G. Wilkinson,⁵⁷ M. Wilkinson,⁶¹ M. Williams,⁵⁶ M. P. Williams,⁴⁷ M. Williams,⁵⁸ T. Williams,⁴⁷ F. F. Wilson,^{51,40} J. Wimberley,⁶⁰ M. Winn,⁷ J. Wishahi,¹⁰ W. Wislicki,²⁹ M. Witek,²⁷ G. Wormser,⁷ S. A. Wotton,⁴⁹ K. Wraight,⁵³ K. Wyllie,⁴⁰ Y. Xie,⁶⁵ M. Xu,⁶⁵ Z. Xu,⁴ Z. Yang,³ Z. Yang,⁶⁰ Y. Yao,⁶¹ H. Yin,⁶⁵ J. Yu,⁶⁵

X. Yuan,⁶¹ O. Yushchenko,³⁷ K. A. Zarebski,⁴⁷ M. Zavertyaev,^{11,c} L. Zhang,³ Y. Zhang,⁷ A. Zhelezov,¹² Y. Zheng,⁶³
 X. Zhu,³ V. Zhukov,³³ J. B. Zonneveld,⁵² and S. Zucchelli¹⁵

(LHCb collaboration)

- ¹*Centro Brasileiro de Pesquisas Físicas (CBPF), Rio de Janeiro, Brazil*
²*Universidade Federal do Rio de Janeiro (UFRJ), Rio de Janeiro, Brazil*
³*Center for High Energy Physics, Tsinghua University, Beijing, China*
⁴*LAPP, Université Savoie Mont-Blanc, CNRS/IN2P3, Annecy-Le-Vieux, France*
⁵*Clermont Université, Université Blaise Pascal, CNRS/IN2P3, LPC, Clermont-Ferrand, France*
⁶*Aix Marseille Univ, CNRS/IN2P3, CPPM, Marseille, France*
⁷*LAL, Université Paris-Sud, CNRS/IN2P3, Orsay, France*
⁸*LPNHE, Université Pierre et Marie Curie, Université Paris Diderot, CNRS/IN2P3, Paris, France*
⁹*I. Physikalisches Institut, RWTH Aachen University, Aachen, Germany*
¹⁰*Fakultät Physik, Technische Universität Dortmund, Dortmund, Germany*
¹¹*Max-Planck-Institut für Kernphysik (MPIK), Heidelberg, Germany*
¹²*Physikalisches Institut, Ruprecht-Karls-Universität Heidelberg, Heidelberg, Germany*
¹³*School of Physics, University College Dublin, Dublin, Ireland*
¹⁴*Sezione INFN di Bari, Bari, Italy*
¹⁵*Sezione INFN di Bologna, Bologna, Italy*
¹⁶*Sezione INFN di Cagliari, Cagliari, Italy*
¹⁷*Università e INFN, Ferrara, Ferrara, Italy*
¹⁸*Sezione INFN di Firenze, Firenze, Italy*
¹⁹*Laboratori Nazionali dell'INFN di Frascati, Frascati, Italy*
²⁰*Sezione INFN di Genova, Genova, Italy*
²¹*Università & INFN, Milano-Bicocca, Milano, Italy*
²²*Sezione di Milano, Milano, Italy*
²³*Sezione INFN di Padova, Padova, Italy*
²⁴*Sezione INFN di Pisa, Pisa, Italy*
²⁵*Sezione INFN di Roma Tor Vergata, Roma, Italy*
²⁶*Sezione INFN di Roma La Sapienza, Roma, Italy*
²⁷*Henryk Niewodniczanski Institute of Nuclear Physics Polish Academy of Sciences, Kraków, Poland*
²⁸*AGH-University of Science and Technology, Faculty of Physics and Applied Computer Science, Kraków, Poland*
²⁹*National Center for Nuclear Research (NCBJ), Warsaw, Poland*
³⁰*Horia Hulubei National Institute of Physics and Nuclear Engineering, Bucharest-Magurele, Romania*
³¹*Petersburg Nuclear Physics Institute (PNPI), Gatchina, Russia*
³²*Institute of Theoretical and Experimental Physics (ITEP), Moscow, Russia*
³³*Institute of Nuclear Physics, Moscow State University (SINP MSU), Moscow, Russia*
³⁴*Institute for Nuclear Research of the Russian Academy of Sciences (INR RAN), Moscow, Russia*
³⁵*Yandex School of Data Analysis, Moscow, Russia*
³⁶*Budker Institute of Nuclear Physics (SB RAS), Novosibirsk, Russia*
³⁷*Institute for High Energy Physics (IHEP), Protvino, Russia*
³⁸*ICCUB, Universitat de Barcelona, Barcelona, Spain*
³⁹*Universidad de Santiago de Compostela, Santiago de Compostela, Spain*
⁴⁰*European Organization for Nuclear Research (CERN), Geneva, Switzerland*
⁴¹*Institute of Physics, Ecole Polytechnique Fédérale de Lausanne (EPFL), Lausanne, Switzerland*
⁴²*Physik-Institut, Universität Zürich, Zürich, Switzerland*
⁴³*Nikhef National Institute for Subatomic Physics, Amsterdam, Netherlands*
⁴⁴*Nikhef National Institute for Subatomic Physics and VU University Amsterdam, Amsterdam, Netherlands*
⁴⁵*NSC Kharkiv Institute of Physics and Technology (NSC KIPT), Kharkiv, Ukraine*
⁴⁶*Institute for Nuclear Research of the National Academy of Sciences (KINR), Kyiv, Ukraine*
⁴⁷*University of Birmingham, Birmingham, United Kingdom*
⁴⁸*H.H. Wills Physics Laboratory, University of Bristol, Bristol, United Kingdom*
⁴⁹*Cavendish Laboratory, University of Cambridge, Cambridge, United Kingdom*
⁵⁰*Department of Physics, University of Warwick, Coventry, United Kingdom*
⁵¹*STFC Rutherford Appleton Laboratory, Didcot, United Kingdom*
⁵²*School of Physics and Astronomy, University of Edinburgh, Edinburgh, United Kingdom*
⁵³*School of Physics and Astronomy, University of Glasgow, Glasgow, United Kingdom*

- ⁵⁴*Oliver Lodge Laboratory, University of Liverpool, Liverpool, United Kingdom*
⁵⁵*Imperial College London, London, United Kingdom*
⁵⁶*School of Physics and Astronomy, University of Manchester, Manchester, United Kingdom*
⁵⁷*Department of Physics, University of Oxford, Oxford, United Kingdom*
⁵⁸*Massachusetts Institute of Technology, Cambridge, Massachusetts, USA*
⁵⁹*University of Cincinnati, Cincinnati, Ohio, USA*
⁶⁰*University of Maryland, College Park, Maryland, USA*
⁶¹*Syracuse University, Syracuse, New York, USA*
⁶²*Pontifícia Universidade Católica do Rio de Janeiro (PUC-Rio), Rio de Janeiro, Brazil, associated to Universidade Federal do Rio de Janeiro (UFRJ), Rio de Janeiro, Brazil*
⁶³*University of Chinese Academy of Sciences, Beijing, China, associated to Center for High Energy Physics, Tsinghua University, Beijing, China*
⁶⁴*School of Physics and Technology, Wuhan University, Wuhan, China, associated to Center for High Energy Physics, Tsinghua University, Beijing, China*
⁶⁵*Institute of Particle Physics, Central China Normal University, Wuhan, Hubei, China, associated to Center for High Energy Physics, Tsinghua University, Beijing, China*
⁶⁶*Departamento de Física, Universidad Nacional de Colombia, Bogota, Colombia, associated to LPNHE, Université Pierre et Marie Curie, Université Paris Diderot, CNRS/IN2P3, Paris, France*
⁶⁷*Institut für Physik, Universität Rostock, Rostock, Germany, associated to Physikalisches Institut, Ruprecht-Karls-Universität Heidelberg, Heidelberg, Germany*
⁶⁸*National Research Centre Kurchatov Institute, Moscow, Russia, associated to Institute of Theoretical and Experimental Physics (ITEP), Moscow, Russia*
⁶⁹*National Research Tomsk Polytechnic University, Tomsk, Russia, associated to Institute of Theoretical and Experimental Physics (ITEP), Moscow, Russia*
⁷⁰*Instituto de Física Corpuscular, Centro Mixto Universidad de Valencia-CSIC, Valencia, Spain, associated to ICCUB, Universitat de Barcelona, Barcelona, Spain*
⁷¹*Van Swinderen Institute, University of Groningen, Groningen, The Netherlands, associated to Nikhef National Institute for Subatomic Physics, Amsterdam, Netherlands*

[†]Deceased.

^aUniversidade Federal do Triângulo Mineiro (UFTM), Uberaba-MG, Brazil.

^bLaboratoire Leprince-Ringuet, Palaiseau, France.

^cP.N. Lebedev Physical Institute, Russian Academy of Science (LPI RAS), Moscow, Russia.

^dUniversità di Bari, Bari, Italy.

^eUniversità di Bologna, Bologna, Italy.

^fUniversità di Cagliari, Cagliari, Italy.

^gUniversità di Ferrara, Ferrara, Italy.

^hUniversità di Genova, Genova, Italy.

ⁱUniversità di Milano Bicocca, Milano, Italy.

^jUniversità di Roma Tor Vergata, Roma, Italy.

^kUniversità di Roma La Sapienza, Roma, Italy.

^lAGH-University of Science and Technology, Faculty of Computer Science, Electronics and Telecommunications, Kraków, Poland.

^mLIFAELS, La Salle, Universitat Ramon Llull, Barcelona, Spain.

ⁿHanoi University of Science, Hanoi, Vietnam.

^oUniversità di Padova, Padova, Italy.

^pUniversità di Pisa, Pisa, Italy.

^qUniversità degli Studi di Milano, Milano, Italy.

^rUniversità di Urbino, Urbino, Italy.

^sUniversità della Basilicata, Potenza, Italy.

^tScuola Normale Superiore, Pisa, Italy.

^uUniversità di Modena e Reggio Emilia, Modena, Italy.

^vIligan Institute of Technology (IIT), Iligan, Philippines.

^wNovosibirsk State University, Novosibirsk, Russia.